

DESIGN OF AN AUTOMOTIVE HV ISOLATED FLYBACK CONVERTER

RISHABH JAIN '26

ADVISOR: MINJIE CHEN

SUBMITTED IN PARTIAL FULFILLMENT

OF THE REQUIREMENTS FOR THE DEGREE OF

BACHELOR OF SCIENCE IN ENGINEERING

DEPARTMENT OF ELECTRICAL AND COMPUTER ENGINEERING

PRINCETON UNIVERSITY

DECEMBER 13 2024

I hereby declare that this Independent Work report represents my own work in accordance with University regulations.

I hereby declare that this Independent Work report does not include regulated human subjects research.

I hereby declare that this Independent Work report does not include regulated animal subjects research.

Rishabh Jain '26

Design of an Automotive HV Isolated Flyback Converter

Rishabh Jain '26

Abstract

This report presents the design and assembly of an isolated high-voltage (HV) DC-DC flyback converter for Princeton's Formula Electric MK3 vehicle. The converter is designed to power the Tractive System Active Light (TSAL) and accumulator indicator light, adhering to both Formula SAE (FSAE) and Formula Hybrid+Electric (FH+E) rules. Key design considerations include a wide input voltage range (60–600 V), galvanic isolation, compactness, and efficiency. A comprehensive approach was taken for each subsystem, spanning input protections, EMI filtering, and component selection. The Analog Devices LT8316 flyback controller was selected for its wide-input range, automotive-grade reliability, and compact design. Simulation results in PLECS was conducted to validate certain aspects of the design such as the EMI filter. Physical assembly of the design was completed, but testing to validate the design and evaluate efficiency remains. This work marks a significant step toward enabling Princeton Racing Electric's MK3 vehicle to pass inspection and compete in dynamic events.

Acknowledgements

I would like to express my gratitude to my adviser, Dr. Minjie Chen. Your teachings have been invaluable in shaping me into a better electrical engineer. I would also like to thank my second reader, Dr. Hossein Valavi, for taking the time to review my work and supporting my academic pursuits across all my classes. You have been a fantastic mentor.

I am especially grateful to my Princeton Racing Electric teammates, Daniel Simone and Stephane Morel, for their unwavering support throughout this project. I would often pester them with questions over slack or in the garage and would never fail to learn something new. The two of them have taught me so much about practical engineering and I will forever be grateful.

This work would not have been possible without the generous financial support provided by the School of Engineering and Applied Science (SEAS) through the Lidow Fund and the ECE Department. I am also grateful for the Princeton PowerLab and ECE undergraduate lab for allowing me to use their facilities. Thank you as well to Jake Rizzo and Jocelyn Law of the ECE Purchasing Office for processing my countless orders.

Contents

Abstract	iii
Acknowledgements	iv
List of Tables	viii
List of Figures	ix
1 Background	1
1.1 Electric Vehicle Industry	1
1.2 Formula Electric and Princeton	3
1.3 Rules & Standards	5
1.4 Previous Work	9
1.5 Design Goals	11
2 Design	12
2.1 Design Approach	12
2.2 Topology Selection	14
2.2.1 Push/Pull Converter	14
2.2.2 LLC Resonant Converter	15
2.2.3 Flyback Converter	15
2.3 Subsystem Overview	16
2.3.1 TSAL design	16
2.4 Input Protections	17

2.5	Input EMI Filter	18
2.6	Flyback Controller (LT8316)	20
2.6.1	Voltage Input with Zener Diodes	21
2.6.2	Pin Configuration	21
2.6.3	Transformer Selection	26
2.6.4	Snubber Circuit	27
2.6.5	EMI Output Filter	28
2.6.6	Y Capacitors	29
2.7	555 Timer	31
2.8	LED Driver	32
2.9	Output Connector and Fuse	32
3	Layout and Assembly	33
3.1	Layout	33
3.1.1	Trace Widths	34
3.1.2	Creepage Distance	35
3.2	Fabrication and Assembly	35
3.2.1	Mistakes	36
4	Conclusion	38
A	Documentation	40
B	Schematics	41
C	Simulations	45
D	PCB Layout and Assembly	46
E	Bill of Materials	48

List of Tables

1.1	Comparison of battery pack voltages and chemistries of different manufacturers and some of their most popular cars.	3
1.2	Minimum Spacing Requirements for Vehicle TS Voltage for both FH+E and FSAE. Integrated circuits such as optocouplers are exempt to this rule if they meet isolation requirements.	8
2.1	Comparison of accumulator voltages and TSAL/Indicator Light Solutions across different universities and their respective results.	13
2.2	Predesigned Transformer Specifications for the LT8316 Flyback Converter	27
2.3	Frequency vs. Interwinding Capacitance with a drive voltage of 5Vpp.	30
3.1	Creepage Distance Constraints	35

List of Figures

1.1	Quarterly sales in electric vehicles from 2021 to Q1 of 2024 split across different regions of the world.	2
1.2	Princeton's all-electric MK2B formula car from 2024 being tested.	3
1.3	A request to FH+E was made and approved to adjust the rules in regards to the lower input range of when the indicators need to turn on.	10
2.1	Illini Electric Motorsports (left) and Wisconsin Racing's (right) approaches to powering their TSAL. Both make use of isolated signal converters, one with an optocoupler (left) and one with a voltage transducer (right).	12
2.2	Block diagram of major subsystems. Note that each bounding box is one printed circuit board (PCB) and is what all of Chapter 2 describes.	17
2.3	A red TSAL PCB designed and assembled by Misael Rosero '27	17
2.4	Bode plot of perturbation towards the LT8316 controller (left) and bode plot of perturbation from LT8316 controller towards the rest of the car (right).	19
2.5	A picture of the FE package of the LT8316 flyback controller. Note pin 21 is an exposed GND pad and also the spacing between VIN and the other pins to increase creepage distance.	25
2.6	Effect of different types of snubbers on the SW Pin's flyback waveform.	27

2.7 Experimental setup (left) and circuit (right) to measure the interwinding capacitance of the 750317464 transformer.	29
3.1 The 3D representation of the PCB with all CAD models for components present.	33
3.2 The assembled DC-DC converter.	36
B.1 An overall schematic of the entire LT8316 flyback converter to power the TSAL and accumulator indicator light.	41
B.2 A schematic of the various input protections of this board.	42
B.3 A schematic of the input EMI filter on this board.	42
B.4 A schematic of the Analog Devices LT8316 flyback controller as used in the DC-DC converter.	43
B.5 A schematic of the BD9555FVM-CGTR 555 Timer.	43
B.6 A schematic of the MPQ24833-BGN-AEC1-Z LED Driver.	44
B.7 A schematic of the output connector and fuse.	44
C.1 Simulation setup in PLECS of the EMI Input Filter's behavior from a perturbation from something like the motor controllers.	45
C.2 Simulation setup in PLECS of the EMI Input Filter's behavior from a perturbation on the flipped side from the switching of the LT8316 controller.	45
D.1 The regional split of the 3D representation of the PCB with all CAD models for components present.	46
D.2 The top copper layer of the PCB.	47
D.3 The bottom copper layer of the PCB.	47

Chapter 1

Background

1.1 Electric Vehicle Industry

Electric vehicles are rapidly gaining widespread adoption among consumers all over the world. In 2023, global electric car sales were at 14 million units making the entire global electric fleet to around 40 million cars with major markets in China, Europe and the United States. Experts project in 2024 that electric car sales could reach 17 million units and account for more than one in five cars sold worldwide as shown by Figure 1.1 [1]. Electric vehicle growth is not limited to just commercial cars or trucks. Even the electrification of public transport is being adopted as seen with Princeton unveiling a new electric bus fleet in November of 2023 [2].

This growth is significantly driven by increased competition among electric vehicle manufacturers, favorable policies, and, most notably, technological advancements. The electric vehicle industry has seen significant advancements in high voltage (HV) powertrains, driven by innovations in battery chemistry, motor controllers, and motors. In battery technology, the development of better lithium-ion batteries with higher energy density and improved charging capabilities has extended driving ranges [1]. The integration of Silicon Carbide (SiC) MOSFETs in power electronics has en-

hanced power efficiency and extended vehicle range due to their capability to operate at higher temperatures [3]. In the realm of electric motors, manufacturers are focusing on next-generation Permanent Magnet Synchronous Motors (PMSMs) and 800V high-voltage architectures [4]. These advancements collectively contribute to the optimization of electric powertrains, resulting in improved vehicle range, performance, and efficiency.

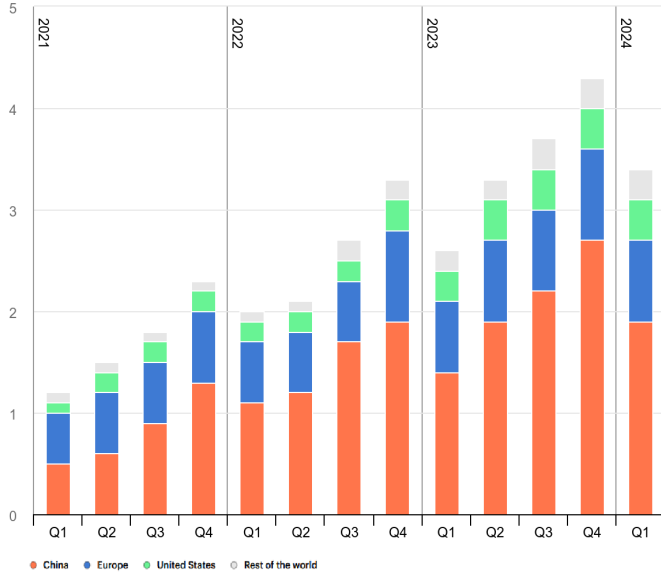


Figure 1.1: Quarterly sales in electric vehicles from 2021 to Q1 of 2024 split across different regions of the world.

As seen in Table 1.1, most manufacturers are using high voltage architectures and lithium-ion battery chemistries of either Nickel Cobalt Aluminium Oxide (NCA), Nickel Manganese Cobalt Oxide (NMC or NCM), and Lithium Iron Phosphate (LFP). Many are even in the process of transitioning their current architectures to even higher voltages. The Porsche Taycan was among the first when it was introduced in 2019 with a 800-volt system that featured an almost entirely custom powertrain including pulse inverters, onboard chargers, battery-management systems (BMS), motors, and more [5]. Ford has also been filing patents to move their powertrain to 800 Volts [6]. This move to higher voltage architectures is happening because it can allow for

Manufacturer	Car Model(s)	Chemistry	Nominal Voltage
Tesla[7][8]	Model S & X	NCA	407V
	Model 3 & Y	NCA/NMC/LFP	355V
	Cybertruck	NMC	700V
Ford[6][9]	F-150 Lightning Mustang Mach-E	NMC/LFP	400V
Hyundai[10]	IONIQ 6 SE	NMC	697V
Rivian[11][12]	R1T	NMC/LFP	400V
Porsche[13][14]	Taycan	NMC/LFP	800V

Table 1.1: Comparison of battery pack voltages and chemistries of different manufacturers and some of their most popular cars.

thinner wiring harnesses (because of less current), lower heat generation, and faster charging as seen with the Taycan [5].

1.2 Formula Electric and Princeton



Figure 1.2: Princeton’s all-electric MK2B formula car from 2024 being tested.

With such widespread adoption of electric vehicles, both hybrid and fully electric collegiate design competitions were created for students to explore EV technology. Two annual events exist: Formula SAE (FSAE) in Michigan and Formula Hybrid+Electric (FH+E) in New Hampshire. Princeton’s own formula electric team,

Princeton Racing Electric, was created back in 2013. Princeton primarily competes at FH+E with the hopes to compete at FSAE in the near future. In 2017, 2018, and 2019, Princeton achieved 2nd place along with IEEE Excellence in Electric Vehicle Engineering awards in 2018 and 2019 [15].

While FH+E typically is stricter in terms of rules, this project aims to be compatible with both sets of rules if the team does end up competing at both events. The competition itself is split into static and dynamic events as described below [16] [17].

Static

Design Students present their design decisions to a panel of experts from industry and academia. The evaluation focuses on the engineering effort, innovative solutions, and the overall quality of their design.

Project Management Students showcase how their project was planned and executed, detailing its scope, timeline, and budget. Deliverables include a written project plan, an interim report, and an oral presentation during the competition.

Dynamic

Acceleration Each car starts from a standstill and is timed over a 75-meter distance to assess its acceleration capabilities.

Autocross Cars are tested for maneuverability and handling on a tight obstacle course that evaluates their acceleration, braking, and cornering performance.

Endurance Vehicles must demonstrate durability by completing a 44-kilometer course, emphasizing efficiency, reliability, and the driver's skill.

Skid Pad (new, FSAE-only) This event measures the car's maximum cornering capability through a figure-eight shaped course, testing the suspension system and the driver's control.

Unfortunately, for the past few years, Princeton has been unable to compete in dynamic events as we have not properly passed the rigorous inspection process. Part

of the reason for this was the Tractive System Active Light (TSAL). The TSAL is a set of status LEDs located at the top of the car that must blink red whenever high voltage is present outside the accumulator and acts as a visual safety indicator to anyone around the vehicle. The MK2 car, shown in Figure 1.2, relies on a 120V architecture and failed to compete in dynamic events in both 2023 and 2024 at FH+E. In 2024, this was primarily due to our commercial off-the-shelf (COTS) DC-DC converter introducing unknown noise on our low voltage lines. Our next-generation car, MK3, runs at a higher \sim 600V architecture using 21700 Molicel p42a lithium ion cells graciously donated by Tesla [18]. It is five segments in series, each of which is configured 28s3p. This project describes the design and construction of a high voltage, automotive DC-DC flyback converter and is essential in passing electrical inspection such that we can compete in dynamic events for the future.

1.3 Rules & Standards

There are two main indicators that this DC-DC converter will be used for. The Tractive System Active Light (TSAL), as described earlier, is a status indicator signaling whether the tractive system is energized for movement.

The accumulator indicator light is a light that provides a visual cue about the accumulator's operational status and is located on the side of the accumulator. The important rules for both FSAE and FH+E are described below. For 2025, there were quite a few changes to the TSAL for FSAE especially. Most notably, it must now be amber and has been renamed to the Ready To Move Light (RTML). However, for the remainder of this document, it will be referred to as the TSAL.

FH+E TSAL Rules [19]

EV9.1.1 The car must be equipped with a TSAL mounted under the highest point of the main roll hoop which must be lit and clearly visible any time the

Accumulator Isolation Relay (AIR) coils are energized.

EV9.1.2 The TSAL must be red. Indicators meeting the requirements of FSAE EV6.9 which show green for TS not present are also acceptable.

EV9.1.3 The TSAL must flash continuously with a frequency between 2 Hz and 5 Hz.

EV9.1.8 The TSAL must be lit and clearly visible any time the voltage outside the accumulator containers is above a threshold calculated as the higher value of 60V or 50% of the nominal accumulator voltage. Operation below Vmin is allowed, but the TSAL must extinguish at voltages below 20V. The TSAL system must be powered entirely by the tractive system and must be directly controlled by voltage being present at the output of the accumulator (no software control is permitted).

EV9.1.9 TS wiring and/or voltages must not be present at the TSAL lamps.

Note: This requirement may be met by locating an isolated dc-dc converter inside a TS enclosure, and connecting the output of the dc-dc converter to the lamp. (Because the voltage driving the lamp is considered GLV, one side of the voltage driving the lamps must be ground-referenced by connecting it to the frame in order to comply with EV4.1.4.)

FSAE RTML/TSAL Rules [20]

EV.5.10.2 Each Ready to Move Light (RTML) must be:

- (b) Color: Amber

EV.5.10.2 The RTML must:

- (a) Be directly controlled by the voltage present in the Tractive System using hard wired electronics. Software control is not permitted.
- (b) Flash with a frequency between 2 Hz and 5 Hz with 50% duty cycle when the voltage outside the Accumulator Container(s) exceeds T.9.1.1 (Any voltage more than 60 V DC)

(c) Not do any other functions

FH+E Accumulator Voltage Indicator Rules [19]

EV9.5.1 Any removable accumulator container must have a prominent indicator, such as an LED, that is visible through a closed container that will illuminate whenever a voltage greater than 30 VDC is present at the vehicle side of the AIRs.

EV9.5.2 The accumulator voltage indicator must be directly controlled by voltage present at the container connectors using analog electronics. No software control is permitted.

FSAE Accumulator Voltage Indicator Rules [20]

EV.5.7 Each Accumulator Container must have a prominent indicator when High Voltage T.9.1.1 (Any voltage more than 60 V DC) is present at the vehicle side of the IRs

EV.5.7.2 The voltage being present at the connectors must directly control the Voltage Indicator using hard wired electronics with no software control.

FH+E General Isolation Rules [19]

EV5.1.1 All TS wiring and components must be galvanically (electrically) isolated from GLV by separation and/or insulation.

EV5.1.2 All interaction between TS and GLV must be by means of galvanically isolated devices such as opto-couplers, transformers, digital isolators or isolated dc-dc converters.

EV5.1.4 All isolation devices must be rated for an isolation voltage of at least twice the maximum TS voltage.

EV5.5.1 If tractive system circuits and GLV circuits are on the same circuit board they must be on separate, clearly defined areas of the board. Furthermore, the tractive system and GLV areas must be clearly marked on the PCB.

EV5.5.2 Prototyping boards having plated holes and/or generic conductor pat-

terns may not be used for applications where both GLV and TS circuits are present on the same board. Bare perforated board may be used if the spacing and marking requirements in EV5.5.3 and EV5.5.1 are met, and if the board is removable for inspection.

EV5.5.3 Required spacings between TS and GLV conductors are shown in Table 1.2. If a cut or hole in the PC board is used to allow the “through air” spacing, the cut must not be plated with metal, and the distance around the cut must satisfy the “over surface” spacing requirement. Spacings between TS and GLV conductors on inner layers of PCBs may be reduced to the “through air” spacings.

Max TS Voltage	Over Surface	Through Air	Under Conformal Coating
301-600 V	12.7 mm	9.5 mm	4 mm

Table 1.2: Minimum Spacing Requirements for Vehicle TS Voltage for both FH+E and FSAE. Integrated circuits such as optocouplers are exempt to this rule if they meet isolation requirements.

- (a) Teams must supply high resolution (min. 300 dpi at 1:1) digital photographs of team-designed boards showing:
 - (i) All layers of unpopulated boards (inner layers or top/bottom layers that don't photograph well can be provided as copies of artwork files.)
 - (ii) Both top and bottom of fully populated and soldered boards.

EV5.5.4 If dimensional information is not obvious (i.e. 0.1 in x 0.1 in spacing) then a dimensional reference must be included in the photo. Spare boards should be made available for inspection. Teams should also be prepared to remove boards for direct inspection if asked to do so during the technical inspection.

EV5.5.5 Printed circuit boards located inside the accumulator container and having tractive system connections on them must be fused to limit the power

on the board to 600 watt or less, with the exception of precharge and discharge circuits.

FSAE General Rules [20]

EV.6.5.7 If Tractive System and GLV are on the same circuit board:

- (a) They must be on separate, clearly defined and clearly marked areas of the board
- (b) Required spacing related to the spacing between traces / board areas are as follows in Table 1.2.

EV.6.5.8 Teams must be prepared to show spacing on team built equipment. For inaccessible circuitry, spare boards or appropriate photographs must be available for inspection

When interpreting the rules, I have taken the stricter of any conflicting rules whenever possible. To summarize, the DC-DC converter must be isolated, have a wide input range of 30-600V DC, and convert down to a reasonable voltage, such as 24V. This will power two sets of LEDs: the TSAL/RTML, which is red in FH+E and amber in FSAE, as well as the accumulator voltage indicator. However, a rules exemption was requested and approved to change the input range for FH+E's lower input range of 30V to 60V to be in agreement with FSAE as shown in Figure 1.3. There are additional rules describing creepage and clearance distances between low voltage and high voltage traces which will matter later when laying out the board. There are a few other mechanical and visibility rules as well for the lights that can be found by checking the original documentation [19] [20].

1.4 Previous Work

As previously mentioned, our MK2 architecture ran at 120V. In order to power the TSAL, a COTS Murata IRH-12/21-W80NB-C isolated DC-DC converter was used.

We have harmonized our rules with FSAE 2025 changing FH+E 2025 rules on EV 2.8.3 and EV 9.5.1 from 30 VDC to 60 VDC.

Closed by  Tremont Miao with status of Resolved 10/28/24 13:44

Figure 1.3: A request to FH+E was made and approved to adjust the rules in regards to the lower input range of when the indicators need to turn on.

It has an ultra wide input range of 16 to 160V and outputs 12V. It can also output up to 250W which is plenty for the lights [21]. The 12V powers as TLC555 timer which switches at the appropriate frequency between 2 and 5 Hz (per EV9.1.3 for FH+E and EV.5.10.2b for FSAE) and drives the TSAL via a PMOS transistor.

While the converter does not extinguish exactly below 20V (minimum threshold is 16V) as per EV9.1.8 per FH+E rules, it does satisfy current FSAE rules as there is no extinguish clause. This is because they removed the green functionality that was there prior to the 2025 ruleset which indicated that the tractive system was inactive. Realistically, the difference between extinguishing below 16V and 20V is negligible because pre-charge takes around 250ms so this threshold is surpassed almost instantly.

Additionally, this converter does have the wide input range necessary as it's highest input of 160V is more than enough for our 120V accumulator. It is also important to note that the MK2 car did not have an accumulator indicator light which, while not necessarily caught during electrical inspection in 2024 probably due to a dysfunctional TSAL, is still a rules violation.

Much of the electrical design for our next-generation vehicle, MK3, is still in progress besides the low voltage system's Vehicle Control Unit (VCU). The HV DC-DC converter used by the MK3 VCU is a SynQor MCOTS-B-600-31-HT which outputs 31V and up to 32A maximum. However, this converter is unsuitable for the lights because its input range is 440-700V [22]. In fact, almost no all-in-one commercial alternatives exist for this wide input range and especially the isolated, low power

profile that is required for the LEDs. A comparison on what some of the other teams, who run at these higher voltages, use can be found in Section 2.1.

1.5 Design Goals

This project looks to design, manufacture, and test an isolated DC-DC flyback converter for Princeton’s own formula electric MK3 car. With the requirements set out in Section 1.3, the overall goals of this design project are to be rules compliant and safe, compact, and efficient.

The FSAE and FH+E tournaments each have their respective set of rules that are necessary to ensure the safety of both students, drivers, and competition staff. This project looks to follow both sets of rules in the hopes of Princeton competing at both competitions’ dynamic events in the future. Additionally, the converter must have the necessary safety features such as overtemperature, overcurrent, overvoltage, undervoltage, and short circuit protection.

The design must be compact due to the limited space within the car’s accumulator. Within the accumulator resides boards for pre-charge control circuitry, battery management systems for each segment, along with isolation relays and the high voltage disconnect. Thus, the overall space was 6” x 2.25” with the tallest component at 1.3”.

While the peak power drawn by this converter is only around 6.24 watts, optimizing its efficiency remains a goal of this project. Although the energy savings from improving the converter’s efficiency may be very small relative to the total power consumption of the vehicle, the TSAL and accumulator indicator light operates continuously, and minimizing unnecessary energy losses aligns with the broader objective of maximizing overall system efficiency, as discussed in Section 1.2.

Chapter 2

Design

2.1 Design Approach

There were multiple approaches considered to solving this problem. Other teams across the country use a variety of techniques to power their indicators as seen in Table 2.1. One popular one among top performing teams was using some sort of tractive system referenced voltage source (such as a depletion mode zener diode or a transducer) and then an isolated DC-DC signal converter (optocoupler or digital isolator) to determine whether or not to power the TSAL from LV. This can be seen in Figure 2.1 [23][24].

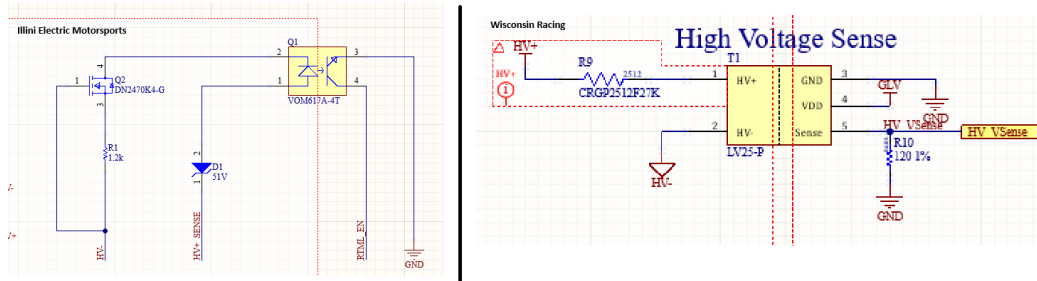


Figure 2.1: Illini Electric Motorsports (left) and Wisconsin Racing's (right) approaches to powering their TSAL. Both make use of isolated signal converters, one with an optocoupler (left) and one with a voltage transducer (right).

An issue that can arise with this is if the LV battery is disconnected, say from a crash, the TSAL would shut off and there could still be high voltage present which is dangerous to volunteers on the track during competition. This can happen if the contactors of the Accumulator Isolation Relays (AIRs) are welded shut.

Other options include using a switched mode power supply (SMPS). For example, one German team uses a non-isolated buck converter such as the VIPER06 to convert from a theoretical maximum of say 800V to 12V and then an isolated 12V to 5V converter. However, efficiency of this specific method is fairly limited. At 600V and an input power of 5W, the efficiency was only around 50% for that specific implementation [25].

Table 2.1: Comparison of accumulator voltages and TSAL/Indicator Light Solutions across different universities and their respective results.

University	Accumulator Voltage (V)	TSAL/Indicator Light Solution	Competition[26] [27]	Place-ment[26] [27]
Rochester Institute of Technology[28]	596	LV Optocouplers	1st in FSAE Electric 2024	
University of Akron[29]	420	LV Signal Converter	3rd in FH+E Electric 2024	
Carnegie Mellon University[30]	600	Flyback Converter	2nd in FH+E Electric 2024	
University of Illinois Urbana-Champaign[23]	600	LV Optocouplers	7th in FSAE Electric 2024	
University of Wisconsin-Madison[24]	300	LV Transducer	3rd in FSAE Electric 2024	

In order to achieve such a wide input range with an isolated converter topology, or-ing converters was considered in what is known as split-rail approaches. In essence, one converter could cover the low range (ie 60V-350V) and the other converter could cover the rest (300V-600V) [31]. There should be a small amount of overlap between the two ranges. When the pre-charge up to 600V was completed in around 250ms,

ideally the overvoltage protection (OVP) of the low range converter would kick in. The controller of this converter would be latching instead of auto-restarting such that it would not keep trying to restart the entire time the tractive system is over the 300V threshold. Another potential solution was some type of voltage-clamping circuit to protect the low range converter. It works by clamping the voltage to a level below the maximum operating voltage of the low range converter but still above the minimum operating voltage of the high range converter (i.e. 325V). However, this pre-charge time of 250ms was estimated based on the load of motor controllers. The TSAL and accumulator indicator light must both work when the motor controllers are disconnected as well and thus the pre-charge time is essentially instant. While the OVP, voltage clamping circuits, or even a resettable fuse should be capable of protecting from sudden transients, this idea was eventually abandoned. In the end, a SMPS flyback converter design was selected and is discussed in comparison with other DC-DC topologies in Section 2.2.

2.2 Topology Selection

One of the most important initial steps is selecting a topology based on our requirements described earlier in Section 1.3. To reiterate, the key characteristics are the wide-input range (60-600V), isolation requirement, compactness, and efficiency.

2.2.1 Push/Pull Converter

Push pull converters use transformer action to transfer power from the primary side to the secondary side. Specifically, it has two center taps on the input and output size and thus has four different windings. Since it uses two switches in alternating cycles, it can produce a continuous output current which produces less EMI and smoother waveforms. It also has lower peak currents because there is very little dead

time and thus it has lower conduction losses [32].

2.2.2 LLC Resonant Converter

An LLC resonant converter also uses transformer action to transfer power from the primary side to the secondary side and can also produce a continuous output current. It has one center tap and thus three windings and also requires careful selection of the the inductors and capacitor. It can come in either a half-bridge configuration with two MOSFETs or full-bridge with four MOSFETs [33]. However, it is not best suited for a wide input voltage range. Additionally, after looking for controllers on sites like digikey, an external supply voltage for the control logic is necessary [34]. If this is powered by an LV battery, it violates the rules. If it is powered by another DC-DC converter, well we have solved our problem already then.

2.2.3 Flyback Converter

The flyback topology uses a single MOSFET and stores energy in an inductor during one part of the cycle and transfers it to the load during the second part of the cycle. This results in a discontinuous current (but continuous output voltage) which is not great in terms of EMI and uneven waveforms [32]. It uses a combination of pulse-width modulation (PWM) and the turns ratio of a transformer to step down the voltage.

It is important to note that TI's Webench Power Designer was also consulted during the initial stages of the project. While it was able to produce a few designs, often the topologies it produced such as phase shifted full bridge or LLC resonant had large Bill of Material (BOM) counts and thus large footprints. The flyback converters and controllers it selected looked promising initially. However, upon closer inspection, there were unrealistic custom components listed in the BOM or, when correct operating values were selected, temperatures on components such as the MOSFET

would be too high because it was switching too often [35].

In the end, a flyback topology was selected. This is primarily because of controller availability across the wide input range. While push/pull seems favorable, there are no commercially available controllers designed for our requirements. Additionally, flyback is the simplest of the designs which reduces the overall component count and thus helps achieve the goal of compactness.

Specifically, the Analog Device LT8316 Flyback controller was selected because it met all of our initial requirements of having a wide-input range (16V-560V), isolation through a transformer (one primary winding, two secondary windings), compact design, and is fairly efficient.

2.3 Subsystem Overview

The design can be split into a few different subsystems: an input EMI filter, the flyback controller, an output filter, a 555 timer, an LED driver, an output connector for both the TSAL and Accumulator Indicator Light, and fuses as appropriate. Throughout the actual board design and schematic, test points are included at various points to check for things such as continuity for fuses or voltages at certain nodes. Additionally, all resistors and most capacitors were selected to be surface mount devices for ease of soldering through reflow and a smaller footprint to achieve the goal of compactness. All schematics that are referenced in the next sections for the entire board can be found in Appendix B.

2.3.1 TSAL design

The printed circuit board (PCB) for the TSAL was designed by another member of our team, Misael Rosero '27. It features two sets of ten 5050 LEDs in parallel and thus runs at around 24V, given a forward voltage drop of around 2V [36]. It also has

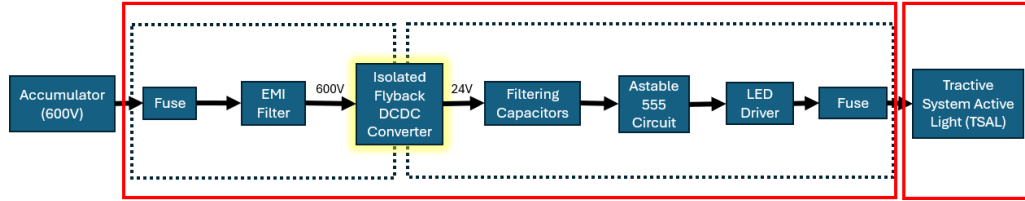


Figure 2.2: Block diagram of major subsystems. Note that each bounding box is one printed circuit board (PCB) and is what all of Chapter 2 describes.

low profile, surface mount WAGO 2059-322/998-403 connectors.

The board is creatively reused as the brake light of the car and can be seen in Figure 2.3. Thus, ten boards were ordered from JLC PCB with six of them populated and one as a demonstration board. The six populated ones are two amber (front TSAL, back TSAL for FSAE), two red (front TSAL, back TSAL for FH+E), one red (brake light), and one for redundancy.



Figure 2.3: A red TSAL PCB designed and assembled by Misael Rosero '27

2.4 Input Protections

The inputs to the DC-DC Converter are through Keystone 7782 terminal blocks that use 1/4" 6-32 screws to secure ring terminals to the board. The wire itself is red and black 600V 22AWG wire donated graciously by Helukabel. Then, it passes through 0ADBC0200-BE, a 200mA 1kV 3AB 3AG cartridge fuse that is stored in

the Littlefuse 03450101H fuseholder [22]. The fuse was sized to trip at over 200mA because only 260mA (120mA from x2 TSAL, 20mA accumulator indicator light) is expected on the output. Thus, at the lowest voltage of 60V, there is still a conversion ratio of 2.5 between output and input (60V/24V) and thus a maximum of 104mA is expected on the input. This fuse satisfies EV5.5.5 in Section 1.3 as it is rated at around 200 watts.

Additionally, a Littlefuse V460LA7P metal-oxide varistor (MOV) with a minimum voltage of 643.5V was used to protect from large transient voltage spikes that are above the converter's maximum input of 644V. In order to provide reverse polarity protection in case wires are connected to the board's terminals in opposite fashion, a 1kV Taiwan Semiconductor Corporation S5MBH diode was included. The schematic for this portion can be seen in Figure B.2.

2.5 Input EMI Filter

A robust input electromagnetic interference (EMI) filter, as shown in Figure B.2 is necessary because of other sources of noise throughout the car such as motors and motor controllers. Specifically, it is important to start filtering at around 10kHz such that at 100kHz, the switching frequency of the motor controllers, the proper attenuation is achieved.

To achieve this, a pi filter was created similar to the MK3 VCU as shown in Figure B.3 and validated with PLECS, a power electronics simulation tool. Four Knowles Syfer 2220Y1K00474KETWS2 0.47 μ F AEC-Q200 1kV X7R ceramic capacitors were used in parallel to filter out high-frequency noise. Then, a Würth Elektronik 7447789270 270 μ H AEC-Q200 shielded inductor was used for differential-mode noise. Additionally, a KEMET C4AQQBU4270A1XJ 2.7 μ F AEC-Q200 1.1kV film capacitor was used for low-frequency noise. Finally, an EPCOS B82724J8162N040 47mH

common-mode choke (CMC) was used to filter out common-mode noise [22].

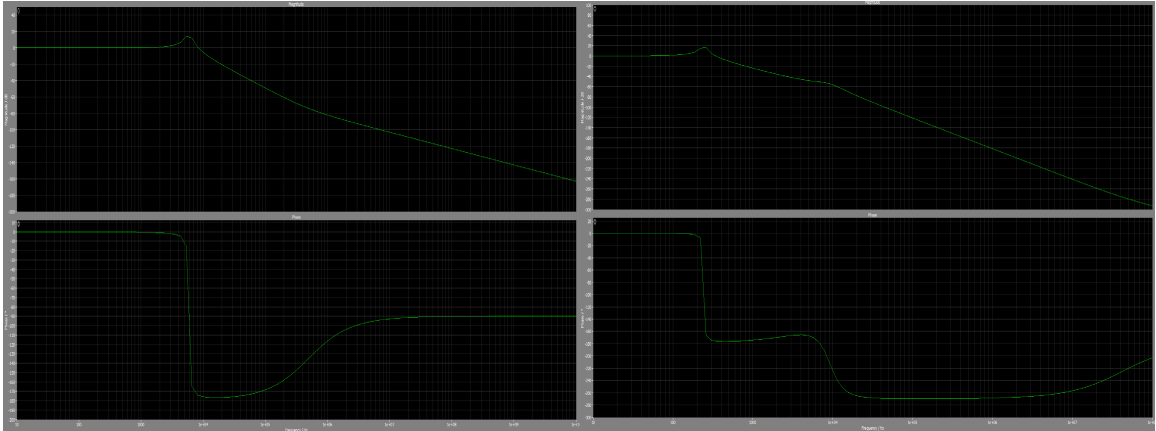


Figure 2.4: Bode plot of perturbation towards the LT8316 controller (left) and bode plot of perturbation from LT8316 controller towards the rest of the car (right).

The PLECS simulation can be seen in Figure 2.4. Images of the PLECS simulation setup can be found in Appendix C and the original PLECS file (version 4.8.9) can be found on the GitHub as described in Appendix A.

A pi filter is a type of low pass filter that works by placing a capacitor on the high-impedance path and an inductor on the low-impedance path. It achieves a better roll off compared to something like a T filter (which instead uses two inductors and a capacitor), but it does have a resonant spike [37]. For the bode plot of the noise towards the converter on the left of Figure 2.4, you can see the cutoff frequency right before 10kHz. You can also see that the slope is initially around -40dB per decade and then past 1MHz, the slope becomes -20dB per decade. At the switching frequency of 100kHz of the motor controllers, a -49 dB attenuation is achieved. Thus, based on the Equation 2.1 and Equation 2.2, if the input voltage were to spike to 700V from the motor controllers (an increase in 100V), the attenuated spike would come out to only be 2.48V.

$$\text{dB} = 20 \cdot \log_{10} \left(\frac{V_{\text{out}}}{V_{\text{in}}} \right) \quad (2.1)$$

$$V_{\text{out}} = V_{\text{in}} \cdot 10^{\frac{\text{dB}}{20}} \quad (2.2)$$

On the right side of Figure 2.4, you can see how noise from the converter affects the rest of the components in the car. The cutoff frequency of this bode plot is at 400Hz and is so low due to the large (47mH) common-mode choke. For this flipped version, we care about the switching frequency of our converter. The LT8316 switches at 3.5kHz in burst mode and up to 140kHz maximum [38]. At 3.5kHz, the attenuation is -45dB while at 140kHz, the attenuation is around -125dB which is plenty. However, there is also a standby mode of the LT8316 where it switches around 220Hz typically. Unfortunately, there is a slight resonant spike at around the standby frequency. This was reasoned to not be an issue because this DC-DC converter at most draws 104mA for barely 250ms of pre-charge and normally 10.4mA at 600V. Furthermore, standby mode is when the switching frequency is even lower to allow for ultralow quiescent power consumption and thus very little noise should be produced by the converter relative to the rest of the car.

2.6 Flyback Controller (LT8316)

As stated earlier in Section 2.2, much of the topology selection is based upon what controllers exist for our input range. The Analog Devices LT8316 was a good candidate for the pre-described conditions. Specifically, it was a flyback controller that had a wide input range of 16V-560V with up to 600V for transients. This input range was also able to be raised to 60V-604V with up to 644V for transients as described in the following section. Additionally, the LT8316 had an automotive-rated (AEC-Q100) variant, came in an integrated circuit (IC) package with extended creepage distance, and no opto-isolator was actually required for feedback regulation [38]. To achieve regulation, a special transformer with one primary and dual secondary windings is

used and talked about in Section 2.6.3. The entire schematic for the LT8316 can be seen in Figure B.4.

2.6.1 Voltage Input with Zener Diodes

The default input voltage range of the LT8316 flyback controller is 16V-560V with up to 600V for transients. Our car, however, will be operating at around 600V continuously. Despite this, there is a way to extend the supply input voltage range for the controller using zener diodes. By placing a Zener diode in series with the V_{IN} pin, the operational range can be extended because the voltage drop across the Zener diode reduces the voltage applied to the chip [39]. Since the default threshold is 16V and the rules from Section 1.3 state that the TSAL and accumulator indicator light need to turn on above 60V, 44V worth of Zener diodes are necessary. Thus, two Taiwan Semiconductor Corporation 1PGSMC5358H AEC-Q101 22V 5W Zener diodes were selected to raise the input voltage range by 44V to meet the minimum required input range of 60V.

2.6.2 Pin Configuration

The following describes the passive components that are used in each pin and each pin's functionality based on the datasheet [38].

EN/UVLO This is the Enable/Undervoltage Lockout (UVLO) Pin. In order to get UVLO functionality (which turns off the IC when the input voltage drops, especially if it drops erratically), a resistor divider is necessary in order to create a voltage on the pin greater than the 1.22V reference voltage. The minimum operating voltage is 60V and thus at 60V, we must be beyond the EN/UVLO threshold of 1.22V in the voltage divider. The formula for the output voltage is given by Equation 2.3

$$V_{\text{out}} = V_{\text{in}} \left[\frac{R_2}{R_1 + R_2} \right] \quad (2.3)$$

The following values were selected

$$V_{\text{in}} = 60 \text{ V}, \quad R_1 = 560 \text{ k}\Omega * 3 = 1.68 \text{ M}\Omega, \quad R_2 = 39 \text{ k}\Omega$$

Thus, the output voltage is approximately $V_{\text{out}} \approx 1.39 \text{ V}$ which is greater than the desired threshold. It is important to note that these resistors are on the high voltage path which is why they are each rated for 500V and the three 560kΩ are used to drop the voltage accordingly.

SENSE This is the current sense pin that is used for current limiting and current-mode control. R_{SNS} needs to be placed between the MOSFET and GND to program the current limit accordingly. Note that in Equation 2.4, V_F represents the forward voltage drop of the output schottky diode (SK320BQ-LTP). Additionally, there is a 100 Ω resistor and a 1000pF capacitor which form an RC filter that smooth the signal going into the SENSE pin by attenuating any high-frequency noise.

$$D = \frac{(V_{\text{OUT}} + V_F) \cdot N_{\text{PS}}}{(V_{\text{OUT}} + V_F) \cdot N_{\text{PS}} + V_{\text{IN}}} \quad (2.4)$$

$$R_{\text{SNS}} = \left(\frac{1 - D_{V_{\text{IN}}(\text{MIN})}}{I_{\text{OUT}}} \right) \cdot \left(\frac{50}{1000} \right) \cdot N_{\text{PS}} \cdot 0.8 \quad (2.5)$$

The following values were selected

$$I_{\text{OUT}} = 260 \text{ mA}, \quad V_{\text{OUT}} = 24 \text{ V}, \quad V_F = 0.82 \text{ V}, \quad N_{\text{PS}} = 4, \quad V_{\text{IN}(\text{MIN})} = 60 \text{ V}$$

Substituting the values into Equations 2.4 and 2.5 to calculate:

$$D = 0.623, \quad R_{SNS} = 0.232 \Omega$$

As a check, the following formula (Equation 2.6) can be used to calculate the maximum current.

$$I_{OUT(MAX)} \approx \frac{100 \text{ mV}}{2 \cdot R_{SNS}} \cdot (1 - D) \cdot N_{PS} \quad (2.6)$$

It is found that $I_{OUT(MAX)}$ is around 325mA which is a 1.25x factor larger than our expected output current of 260mA which gives us a safe margin. In reality, R_{SNS} was selected to be 0.27Ω as per the E12 standard resistor series.

IREG/SS The IREG/SS pin is for current regulation and soft-start. The current is programmed using a resistor and the formula described by Equation 2.7. A capacitor is necessary to implement soft-start, but this was not implemented because soft-start works by gradually increasing the output voltage which helps reduce stress on components. In reality, we want the TSAL and accumulator indicator light activated as soon as high voltage is present, not after some delay. A factor of 1.25 was introduced to provide a safety factor for the maximum output current.

The equation for $R_{IREG/SS}$ is given as:

$$R_{IREG/SS} = \frac{2.5 \text{ M}\Omega \cdot I_{OUT} \cdot R_{SNS}}{N_{PS}} \quad (2.7)$$

The following values were selected

$$I_{OUT} = 260mA * 1.3 \quad R_{SNS} = 0.27\Omega \quad N_{PS} = 8/2$$

Thus, the calculated value is:

$$R_{\text{IREG/SS}} = 95.5 \text{ k}\Omega$$

The actual selected value for $R_{\text{IREG/SS}}$ was $100\text{k}\Omega$ as this follows the standardized E12 resistor series.

V_C This is the loop compensation pin which determines the switching frequency and peak current limit for power delivery. A series RC network is used to stabilize the regulator. In this case, typical values of $R_C = 10\text{k}\Omega$ and $C_C = 220\text{nF}$ were selected.

INTV_{CC} This is the internal gate driver bias voltage. It was bypassed locally with a Samsung Electro-Mechanics CL31B475KBHVPNE 4.7uF 50V X7R ceramic capacitor.

S MODE This is the standby mode pin which was enabled by connecting to INTV_{CC} . This allows the minimum switching frequency to reduce all the way to around 220 Hz and allows ultra-low power consumption at the expense of longer period between samples.

GND This is just ground. The FE package of the LT8316 was selected, specifically the LT8316IFE#WTRPBF variant. This option was lead-free, automotive rated, and also has a large exposed pad (pin 21) connected on the bottom of the package as seen in Figure 2.5. This allows for better thermal dissipation and a more stable ground reference for the IC.

GATE This is the gate driver output of the LT8316 and is connected to the MOSFET through a 20Ω resistor. This resistor is placed at the gate of the MOSFET because the gate to source of a MOSFET can act like a capacitor and thus it limits the inrush current [40]. The MOSFET selected was the STMicroelectronics STD6N90K5 900v 6A N-channel FET.

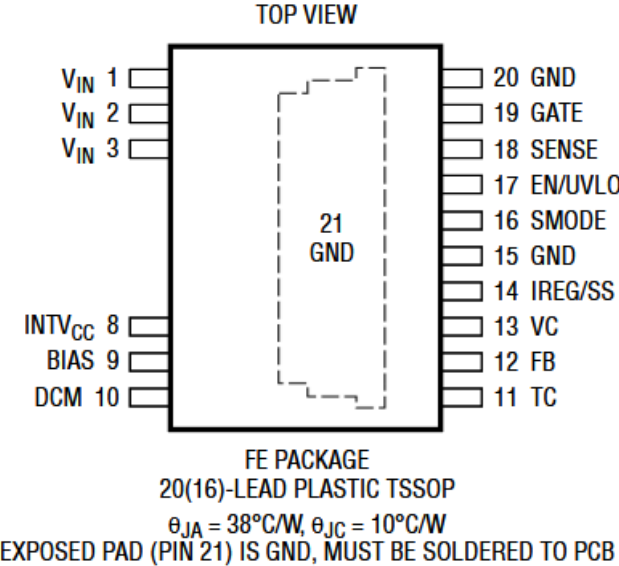


Figure 2.5: A picture of the FE package of the LT8316 flyback controller. Note pin 21 is an exposed GND pad and also the spacing between VIN and the other pins to increase creepage distance.

FB This is the feedback pin where voltage from that tertiary winding is sampled and regulated to equal the 1.22V internal reference voltage. A resistor divider is used to regulate the output voltage and programmed using R_{FB1} and R_{FB2} .

$$V_{\text{OUT}} = \left(1 + \frac{R_{FB2}}{R_{FB1}}\right) \cdot \frac{1.22\text{ V}}{N_{\text{TS}}} - V_F \quad (2.8)$$

$$R_{FB2} = R_{FB1} \cdot \left(\frac{(V_{\text{OUT}} + V_F) \cdot N_{\text{TS}}}{1.22\text{ V}} - 1 \right) \quad (2.9)$$

An R_{FB1} value of $4.99\text{k}\Omega$ was selected as a default value which gives a value for R_{FB1} of $45.77\text{k}\Omega$. To match the E12 standard, a $47\text{k }\Omega$ resistor was selected.

TC This is the temperature compensation pin. This needs to be connected to an appropriate resistor to the feedback (FB) pin.

$$\text{TC}_F = -\frac{\Delta V_{\text{OUT}}}{\Delta T} \quad (2.10)$$

Using the following values from the datasheet for the output schottky diode (the SK320BQ-LTP):

$$\Delta V_{\text{OUT}} = 0.68 - 0.82 \quad \Delta T = 125 - 25$$

We end up getting a TC_F value of -1.4 which can be used in Equation 2.11 to calculate the temperature compensation resistor value R_{TC} of $268\text{k}\Omega$. To match the E12 standard, a $270\text{k }\Omega$ resistor was selected.

$$R_{\text{TC}} = \frac{-R_{\text{FB2}} \cdot 4.1 \text{ mV}/{}^{\circ}\text{C}}{TC_F \cdot N_{\text{TS}}} \quad (2.11)$$

DCM This pin detects discontinuous conduction mode based on the dV/dt of the switching waveform. A resistor and capacitor are connected in series with typical values of R_{DCM} selected as $10\text{k }\Omega$ and C_{DCM} selected as 47pF .

BIAS The bias pin is the unregulated input voltage for the IC that comes from the tertiary winding of the transformer. It is bypassed with a Samsung Electro-Mechanics CL31B475KBHVPNE 4.7uF 50V X7R ceramic capacitor.

2.6.3 Transformer Selection

Picking out the magnetics of a flyback converter is a very important decision. In this case, since we are using the LT8316 flyback controller, we need a transformer that has one primary and two secondary windings. That third winding is necessary to provide feedback to the correct pins as described above. Analog Devices actually collaborated with magnetics manufacturers to create pre-designed flyback transformers that worked with this flyback controller. Out of the predesigned transformers, the Würth Elektronik 750317464 and the Sumida 11328-T080 both meet all of our requirements. They are even reinforced rated rather than functionally isolated which

may meet rule requirements but in actuality are not safe. Detailed specifications about these two transformers can be found in Table 2.2.

Part Number	$L_{\text{PRI}}(\mu\text{H})$	$N_{\text{P}} : N_{\text{S}} : N_{\text{T}}$	Isolation	Vendor	Target Applications
750317464	440	4:1:0.5	Reinforced	Würth Elektronik	100V–600V to 24V/2A
11328-T080	670	4:1:0.5	Reinforced	Sumida	100V–600V to 24V/1.5A

Table 2.2: Predesigned Transformer Specifications for the LT8316 Flyback Converter

Unfortunately, both of these transformers were out of stock on common vendors such as Digi-Key and Mouser. Luckily, thanks to Fred Amori of Sumida and Juliette Arenas of Würth Elektronik, I was able to get samples shipped in time. In the end, Sumida's 11328-T080 transformer was selected. This is because the creepage distance for the 750317464 between HV+ and HV- were quite low (16.7 mils between the pins after following the wiring on the datasheet).

2.6.4 Snubber Circuit

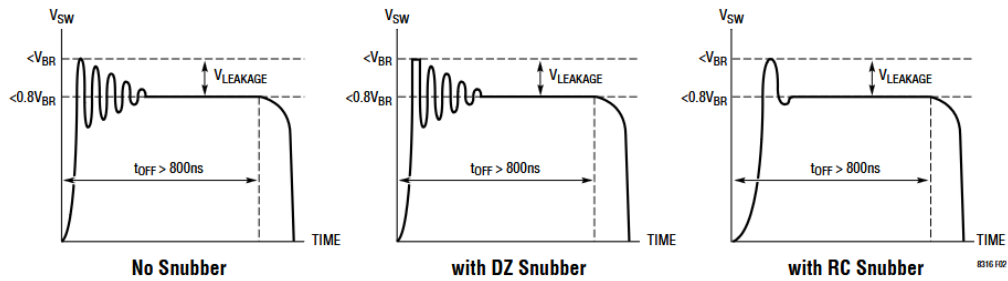


Figure 2.6: Effect of different types of snubbers on the SW Pin's flyback waveform.

Snubbers are essential for flyback converters because of leakage inductances on the primary winding of transformers. It is similar to those kickback diodes motors have because current through an inductor can not instantaneously change. This is because

when the MOSFET turns off, there is a large voltage spike which can exceed the rating of the MOSFET and other components. Additionally, it causes the switching node to ring for some time which is why diode-zener (DZ) or resistor-capacitor (RC) snubbers are useful as shown in Figure 2.6. In this case, a DZ snubber was selected as it ensures a well-defined and consistent clamping voltage and has a higher power efficiency than the RC snubber [38]. A fast-recovery diode with a reverse-voltage rating higher than the max MOSFET drain pin voltage was selected, specifically the onsemi NRVUS1MFA which has a DC Reverse Voltage of 1000 V. The Zener diode chosen was the Vishay SMBJ188A-E3/5B and it was chosen based on a large breakdown voltage and ability to withstand a sufficient power loss.

2.6.5 EMI Output Filter

On the output of the LT8316's transformer's secondary winding, a simple EMI filter was devised. It consists of a Micro Commercial SK320BQ-LTP 200V 3A schot-ky diode that has a forward voltage drop of 0.82V. Additionally, there is a KEMET C1206C102J5RACAUTO 1000pF 50V X7R and two Murata GRT31CR61H106ME01L 10uF 50V X5R ceramic capacitors. While a higher capacitance could reduce the amount of ripple, this was not entirely necessary because this output is getting fed into an LED Driver which is configured in buck/boost mode. Finally, there is a Schaffner RN102-1.5-02-1M6 1.6mH common-mode choke. The choke is necessary because it adds inductance for currents that are unbalanced. These currents can be unbalanced because at the moment that the LT8316 converter switches, everything else in the car (such as the motor controllers or the VCU's SynQor converter) may not switch at that exact time. Thus, by adding inductance, it will make these currents smaller and ring less.

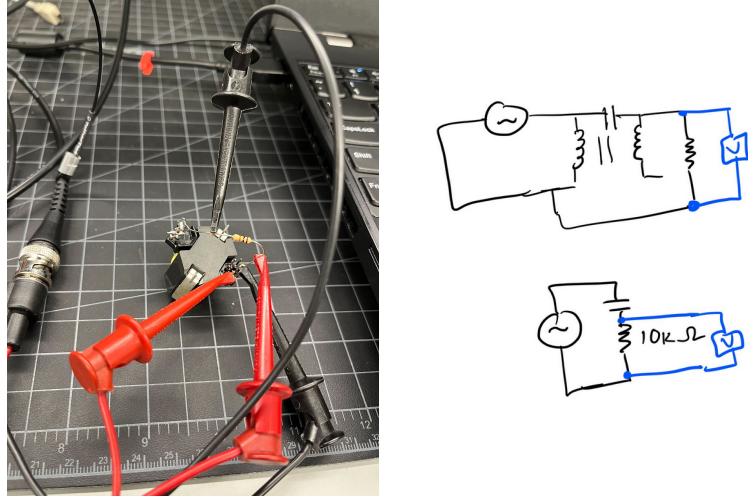


Figure 2.7: Experimental setup (left) and circuit (right) to measure the inter-winding capacitance of the 750317464 transformer.

2.6.6 Y Capacitors

The inter-winding capacitance is the capacitance between the windings of a transformer or inductor. To reduce EMI between HV and LV, Y capacitors with significantly larger capacitance values than the inter-winding capacitance are often required. These Y capacitors help control HV and LV ground currents such as the ones between the motor controllers and accumulator. Thus, the PCB design included a footprint (that met FH+E and FSAE spacing requirements) for a Y capacitor, but the choice to actually populate it can be decided later on based on the presence of EMI. To size the Y capacitor, measurements as shown in Figure 2.7 had to be taken to determine the actual magnitude of the inter-winding capacitance as the datasheets did not include them.

$$V_R = V_{IN} - V_C \quad (2.12)$$

$$V_R = V_{IN} \cdot \frac{R}{R + \frac{1}{2\pi f C}} \quad (2.13)$$

$$C = \frac{1}{2 \cdot \pi \cdot f \cdot R \left(\frac{V_{IN}}{V_R} - 1 \right)} \quad (2.14)$$

Using the fact that the resistor and capacitor form a voltage divider relative to the overall impedance of the circuit, we can calculate the voltage drop across the resistor using Equation 2.13. Then, using the formula in Equation 2.14, one can calculate the inter-winding capacitance knowing the following values. The results are shown in Table 2.3.

$V_{in} = 1.78 \text{ V}(5V_{rms})$, $R = 10 \text{ k}\Omega$, $V_R = \text{from multimeter}$ $f = \text{from function generator}$

Frequency	Inter-winding Capacitance
10 kHz	19 pF
100 kHz	12.5 pF
1 MHz	1.25 pF

Table 2.3: Frequency vs. Interwinding Capacitance with a drive voltage of 5Vpp.

The actual interwinding capacitance from the primary and auxillary winding to the secondary was around 55pF with the drive at 100mV and 100kHz per Wurth Elektronik's engineering team [41]. The experimental values I measured may be lower because they did not include the auxillary winding and it was also at a higher drive voltage. Regardless, this value should be remeasured for Sumida's 11328-T080 going forward. In the end, the KEMET R4Y5I12205000K 2200pF 3kV AEC-Q200 Y1 capacitor was selected. The R4Y series by KEMET has a range of values for Y capacitors for the same footprint which allows modularity going forward.

2.7 555 Timer

A 555 timer is necessary because the TSAL must flash between 2 and 5 Hz with a 50% duty cycle as per FH+E EV9.1.3 and FSAE EV.5.10.2 (b). In order to achieve this, a 555 timer in astable mode can be used. The Rohm Semiconductor BD9555FVM-CGTR was selected because it was the only automotive rated 555 timer that could take 24V as an input [42]. For the V_{IN} pin, there is a CL31B475KBHVPNE 4.7uF 50V X7R ceramic decoupling capacitor to smooth the input voltage out. Additionally, for the DCENB, since we want a PWM output, we must raise it "H" or above 4.4V to a maximum of $V_{IN} + 0.2V$. Thus, a voltage divider was created with a 20k Ω and a 10k Ω resistor. This gives a 1/3 ratio and thus, if $V_{IN} = 24V$, the DCENB pin will be around 8V which is plenty past the threshold of 4.4V.

To configure the actual switching frequency, the formulas shown in Equations 2.15 and 2.16 were used.

$$T_1 = \frac{\Delta V_{CRT} \cdot C_{CRT}}{I_{CRT_SO}} \quad [s] \quad (2.15)$$

$$T_2 = -C_{CRT} \cdot (R_{CRT} + R_D) \cdot \ln \left(\frac{V_{CRT_CHA}}{V_{CRT_DIS}} \right) \quad (2.16)$$

With a 50% duty cycle, note that $T_1 = T_2$ and also that $\ln(\frac{V_{CRT_CHA}}{V_{CRT_DIS}}) = \ln(\frac{1.1}{3})$, $R_D = 50$, and $I_{CRT_SO} = 35\mu A$ based on the datasheet. A final resistance of 54k Ω and capacitance of 1.8uF was calculated. However, a final resistance of 56k Ω and capacitance of 3uF was actually selected. A slightly higher capacitance value was selected because capacitors tend to derate depending on operating voltage and temperatures.

2.8 LED Driver

An LED Driver is necessary to ensure there is a consistent and constant current. This is because if LEDs run for a long time, their resistance changes and that can change how much current they can end up pulling. Thus, the MPQ24833-BGN-AEC1-Z LED Driver was selected as it has a wide operating range and can operate in buck-boost mode [43]. Additionally, it is being used on the next iteration of the MK3 VCU to drive the car's brake light [22]. The LED Driver supports both analog and PWM dimming. In order to get DC dimming, V_{LED_EN} must be over the 1.75V threshold, but below the maximum of 6V and thus a resistor divider was created to generate 5V for the LED_EN signal that goes into the EN/DIM pin. Much of the remaining schematic is based upon the typical buck-boost converter application, except for the feedback pin. A resistor divider with 1Ω and 3.3Ω in parallel was formed for the sense resistor based on Equation 2.17. This gives use an I_{LED} of around 261mA which is very close to our desired current of 260mA.

$$R_{SENSE} = \frac{0.2 \text{ V}}{I_{LED}} \quad (2.17)$$

2.9 Output Connector and Fuse

The Bel Fuse 0ZCF0050FF2C 500mA 60V resettable fuse was selected for it's compactness and automotive rating. The Molex 0015247040 4 position receptacle was selected for it's short height and compactness. This allows two wires to go towards the TSAL and the other two wires to go towards the accumulator indicator light. The APEM Q8F3CXXR24E panel mount red indicator was selected as the accumulator indicator light. This is because it works in a range of 21.6V to 26.4V and has an operating current of 20mA. A diagram of all these components can be seen in Figure B.7.

Chapter 3

Layout and Assembly

3.1 Layout

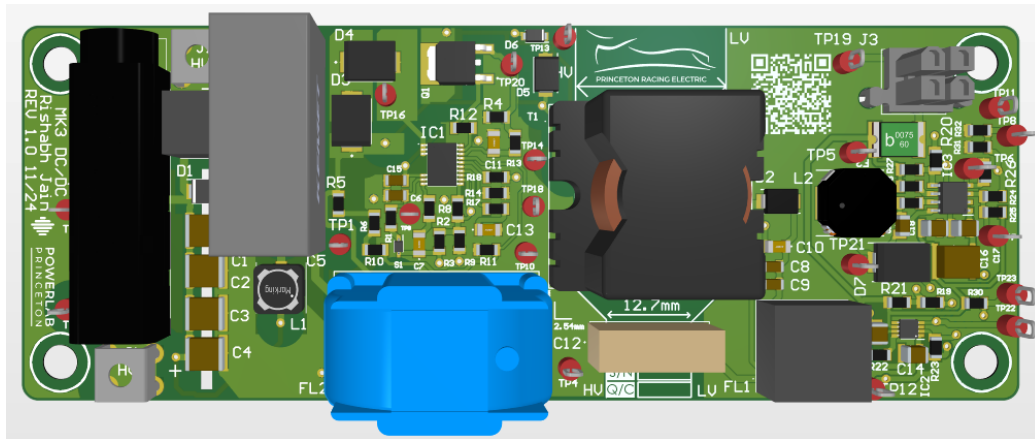


Figure 3.1: The 3D representation of the PCB with all CAD models for components present.

The entire schematic and layout was done using Altium Designer. The actual layout can be seen in Figure 3.1. Some important design decisions that were made was separating out HV from LV as far apart as possible. The majority of the left side of the board deals with HV while the right side of the board deals with LV. Note the various test points across the board. A regional breakdown of the board can

be seen in Appendix D. Additionally, the top copper layer can be seen in Appendix Figure D.2 and the bottom copper layer in Appendix Figure D.3. Further note the board cutouts that were used on the EMI input filter by the capacitors C1, C2, C3, and C4 on the left.

For the 5W input Zener diodes that go into the V_{IN} pins of the LT8316, a large copper pour was created around each of the pads. Additionally, multiple HV and LV ground planes were used to reduce EMI and also for thermal dissipation.

As mentioned earlier, the board was constrained in size due to other boards that reside in the accumulator. Specifically, pre-charge control circuitry, battery management systems for each segment, isolation relays, and the high voltage disconnect. The overall dimensions ended up being 6" x 2.25" with the tallest component being the input common-mode choke (B82724J8162N040) at 1.3". Four 10-24 non plated mounting holes were created in each corner such that the board can stack with other boards within the accumulator.

The silkscreen features logos for Princeton Racing Electric, Princeton PowerLab, a serial number box, a quality control box, a dimensionally accurate reference (for FH+E EV5.5.4), spacing dimensions between HV and LV areas (the transformer and Y capacitor), and a QR code for documentation.

3.1.1 Trace Widths

The maximum expected current draw on this board is around 260mA. Using a PCB trace width calculator, the minimum required trace width in air is under 2 mils [44]. Despite this, trace widths of 25 to 50mil were primarily used across the board with the minimum trace width being 15mil for copper layers as confirmed by the PCB List feature.

3.1.2 Creepage Distance

Creepage distances between HV and LV as per FSAE and FH+E are mentioned in Table 1.2. The over surface minimum distance is 12.7mm. A larger 15mm was selected as shown in Table 3.1. The other values were determined based on IPC-2221B standards and a calculator for it [45] and upsized slightly to allow a larger safety margin.

The exceptions to this are the Y capacitor which is separated by exactly 12.7mm, the LT8316 integrated circuit which already has some pins removed for high voltage spacing as shown in Figure 2.5. Additionally, technically the drain of the STD6N90K5 can be considered high voltage as opposed to its gate signal and source. There is only 1.83mm of separation instead of the desired 3.048mm between these two because of the TO-252-3/DPAK package that the MOSFET comes in.

Name	Priority	Attributes (Distance in mm)
HV to LV	1	Distance constraint 15.0 mm
HV+ to HV-	2	Distance constraint 3.048 mm
HV- Filtered to HV-	4	Distance constraint 0.762 mm
LV+ to LV-	3	Distance constraint 0.254 mm

Table 3.1: Creepage Distance Constraints

3.2 Fabrication and Assembly

The board was sent to Osh Park for fabrication due to both U.S. manufacturing and shorter lead times to try and design and test it within one semester. There was some concern over the fr4 core that JLC PCB uses when dealing with such high voltages which is also why Osh Park was selected.

A final, assembled version of the board can be seen in Figure 3.2. The actual assembly was done using a hot plate in order to solder a majority of the surface mount devices. For the integrated circuits, kapton tape and the precision soldering iron was



Figure 3.2: The assembled DC-DC converter.

used to carefully solder individual pins. The remaining through hole components were soldered on at the end.

3.2.1 Mistakes

There were some mistakes throughout the design and assembly process that are documented below. Some of these have been rectified while others will need to be rectified in a second iteration on this design.

- Osh Park randomly added some non-plated holes sporadically throughout parts of the HV side of the board, suggesting that the NC drill files may have been corrupted.
- The edges of the board from Osh Park were not filed down probably due to the Super Swift service that was selected.
- The incorrect fuseholder knob was ordered (03450121H instead of 03450101H). Thus, the spring had to be tampered with to allow the larger fuse to eventually fit.

- Digi-Key accidentally sent two spools of leaded solder instead of the two R4Y5I12205000K 2200pF Y Capacitors. The Y capacitor was not populated in the assembly picture in Figure 3.2.
- To make the process of ordering resistors simpler, the E12 resistor standard was used so a 1206 resistor series kit could be ordered. However, 0.27 ohms, the value for the sense resistor, was not included in the resistor kit. To fix this in the hopes of preliminary testing, four 1 ohm resistors were stacked vertically in parallel (R4 at the top middle of Figure 3.2).
- The output Schottky diode (SK320BQ-LTP) was accidentally excluded from the BOM. However, two of the LED Driver's diodes (B560C-13-F) were ordered and wires were soldered between the diode and the pads to connect the two.
- It is not necessary for the accumulator indicator light to flash between 2 and 5 Hz and thus it does not need to be connected to the 555 timer at all.
- Another BOM issue involved accidentally editing the comment and not the value so the 3uF capacitor for the 555 timer was not ordered. It is currently replaced with an extra 4.7uF and the resistor was adjusted from 56k to 22k.
- More time needs to be devoted to tracing and debugging the open circuit in the current PCB.

Chapter 4

Conclusion

This paper details the design and assembly of a wide input high voltage DC-DC flyback converter to be used in a formula electric vehicle. It successfully addressed the various challenges of having a wide voltage input range, competition rules, and space constraints. The Analog Devices LT8316 flyback controller was selected and robust EMI filters were designed to protect the converter. Simulations in PLECS confirmed the converter's capability to attenuate noise effectively. This work serves as a foundation for future automotive HV system designs and could be applicable to other formula electric teams especially. Unfortunately, due to the time constraints of a one semester independent work and lead times for ordering components like a PCB, little testing was actually conducted. The most important next step is determining why the converter does not work which I plan to do over Wintersession and continue independently next semester. Many of the preliminary, low hanging fruit design mistakes are listed in Section 3.2.1. Other future improvements to the design are as follows:

- Replacing the S5MBH with a larger footprint diode for reverse protection.
- Fixing the connector for the Molex because it does not positively latch and also the male mating portion touches the fuse (even though it is plastic).

- Dampening the resonant spike that happens at the switching frequency in the EMI input filter
- Fixing the footprint for the test points or ordering different test points such that they can easily snap in and out of the board and are held by friction fit instead of being soldered.
- Simplifying the BOM such that components are not missed as easily
- Stencil perhaps laser cut from thin acrylic for soldering the integrated circuits, especially the LT8316
- Cleaning up the silkscreen because at one point I had accidentally soldered a capacitor to the pads for a resistor because of how dense the board is
- Validation of the circuit's behavior in a software like LTSPICE is another avenue that can be explored.

Appendix A

Documentation

Files and documentation such as the PLECS simulation can be found at the following link: <https://github.com/J-Rishabh/MK3-DC-DC>

Appendix B

Schematics

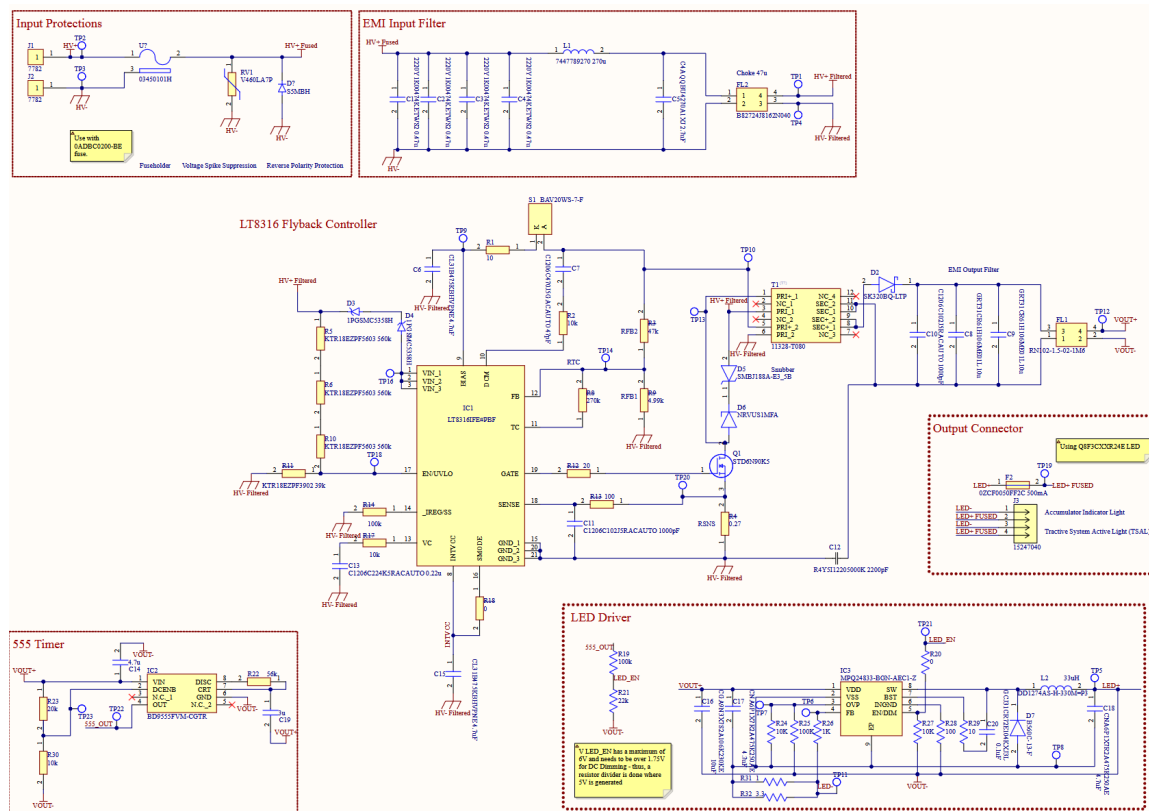


Figure B.1: An overall schematic of the entire LT8316 flyback converter to power the TSAL and accumulator indicator light.

Input Protections

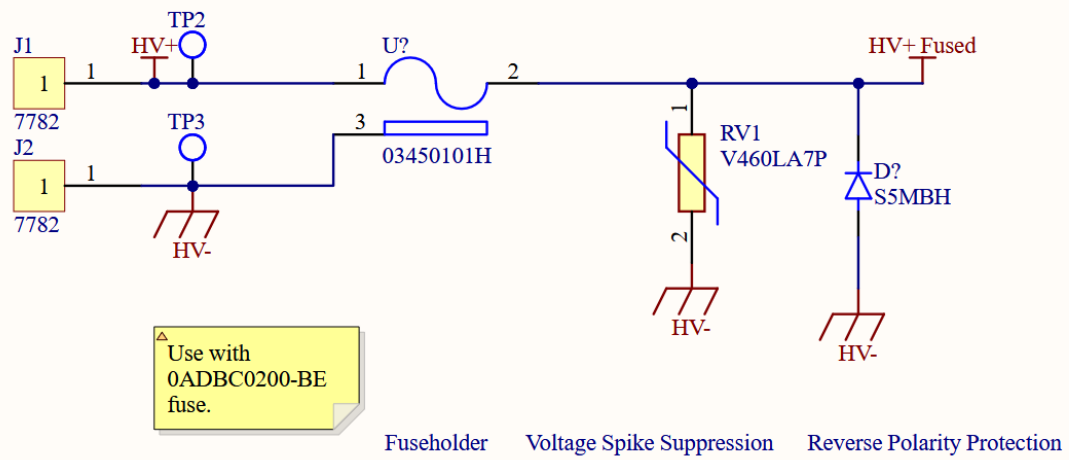


Figure B.2: A schematic of the various input protections of this board.

EMI Input Filter

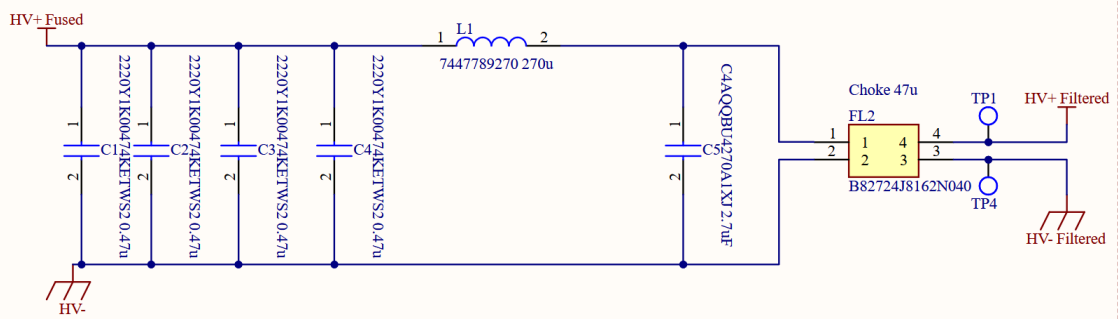


Figure B.3: A schematic of the input EMI filter on this board.

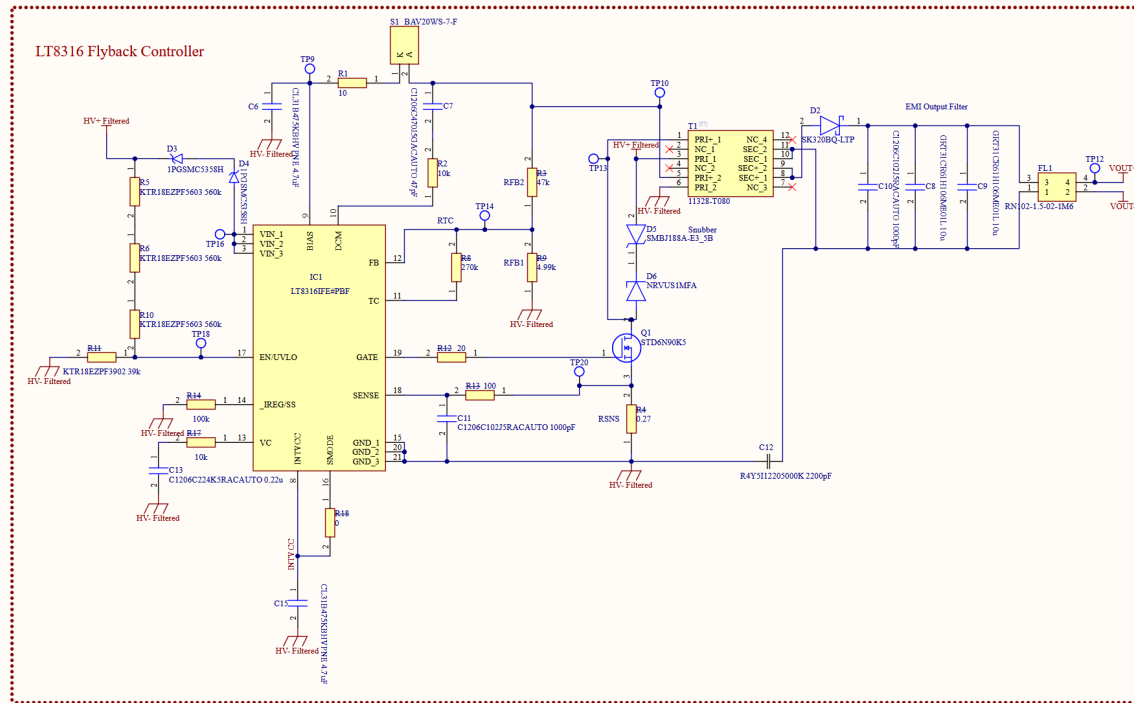


Figure B.4: A schematic of the Analog Devices LT8316 flyback controller as used in the DC-DC converter.

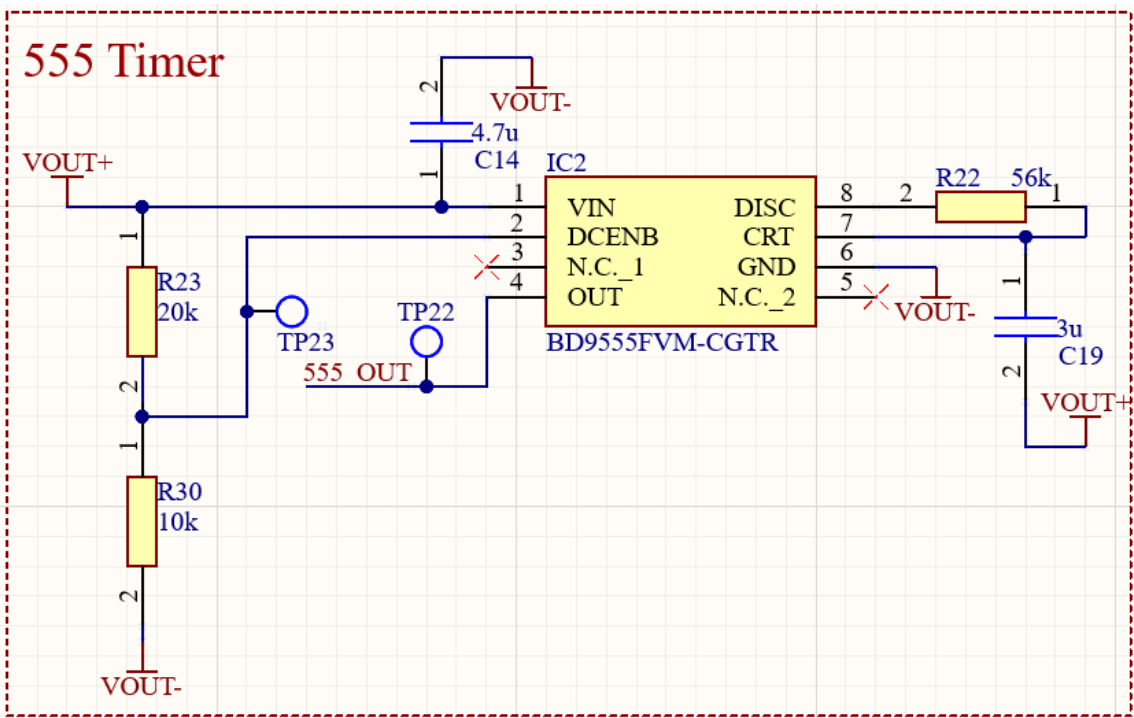


Figure B.5: A schematic of the BD9555FVM-CGTR 555 Timer.

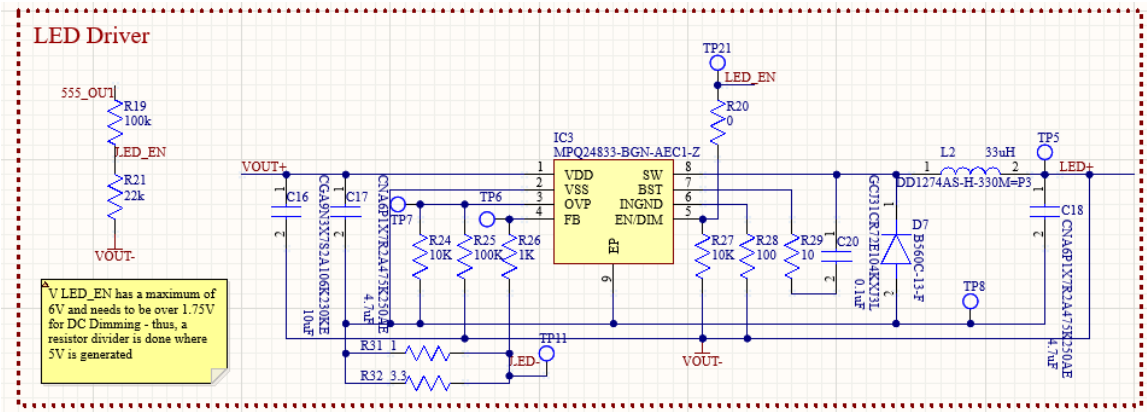


Figure B.6: A schematic of the MPQ24833-BGN-AEC1-Z LED Driver.

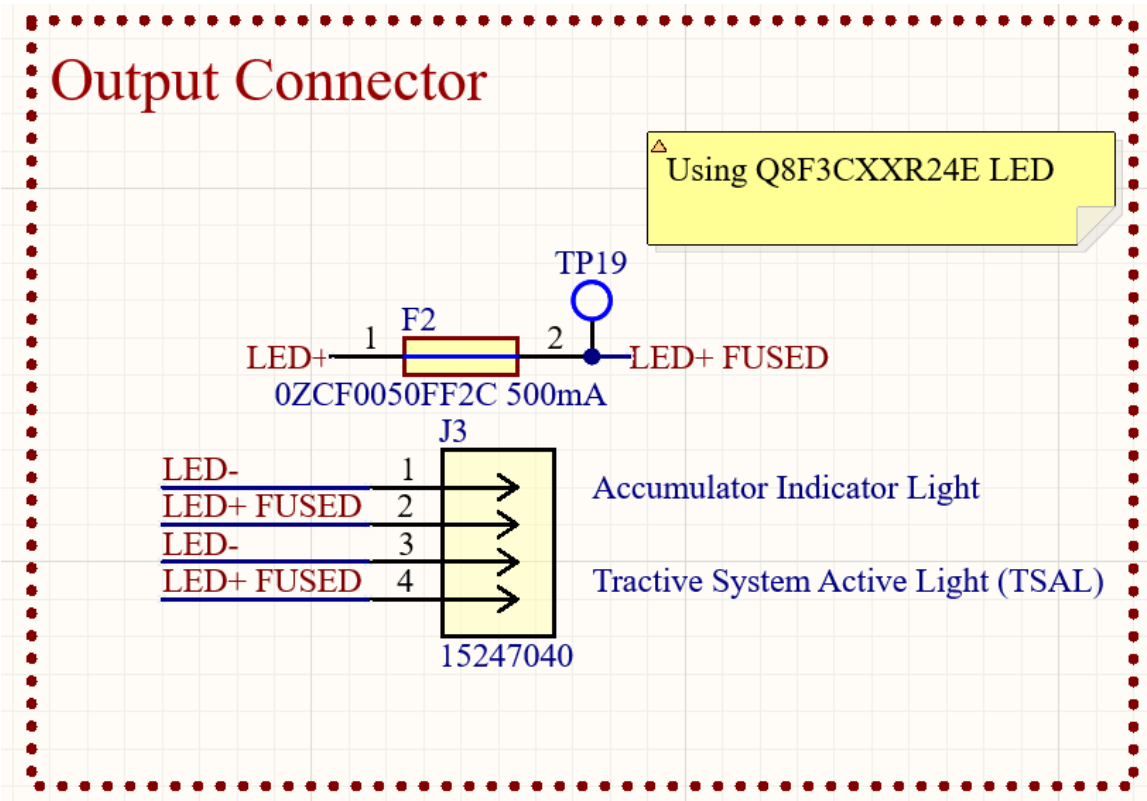


Figure B.7: A schematic of the output connector and fuse.

Appendix C

Simulations

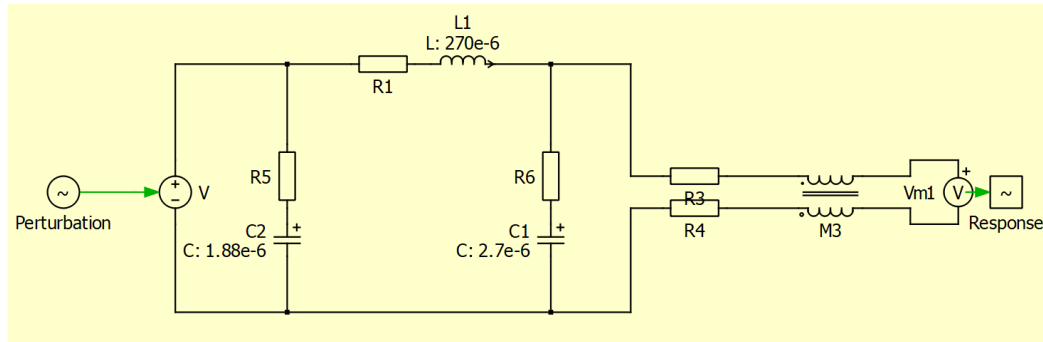


Figure C.1: Simulation setup in PLECS of the EMI Input Filter's behavior from a perturbation from something like the motor controllers.

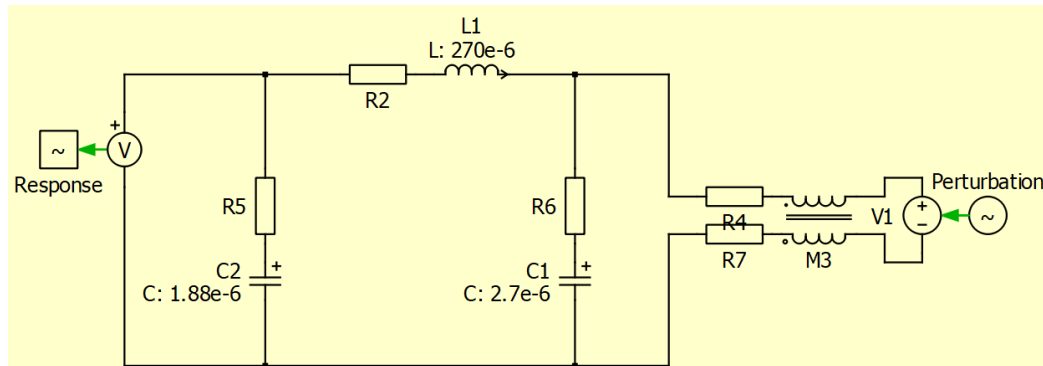


Figure C.2: Simulation setup in PLECS of the EMI Input Filter's behavior from a perturbation on the flipped side from the switching of the LT8316 controller.

Appendix D

PCB Layout and Assembly

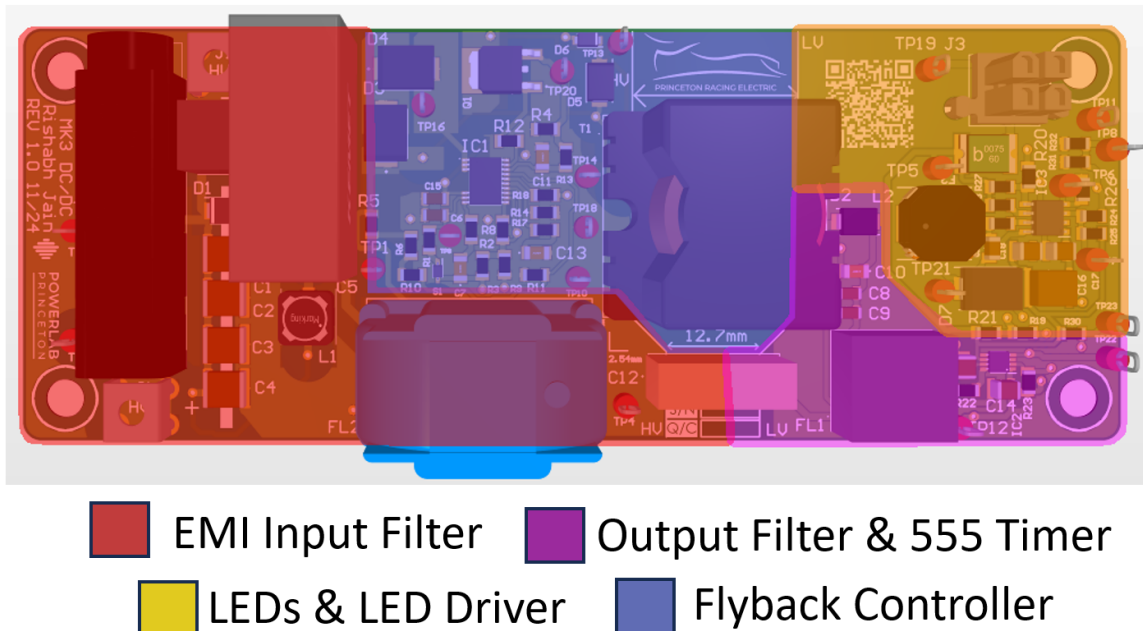


Figure D.1: The regional split of the 3D representation of the PCB with all CAD models for components present.

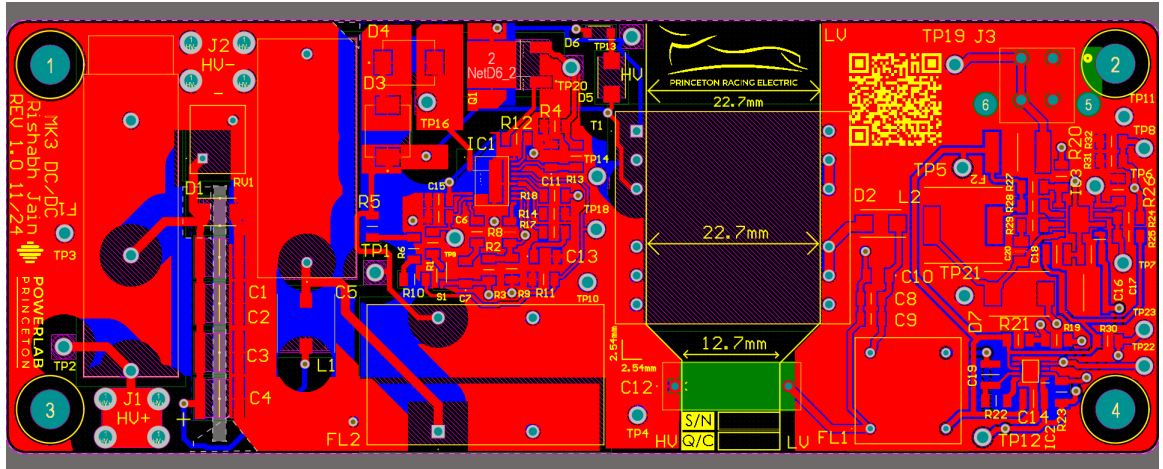


Figure D.2: The top copper layer of the PCB.

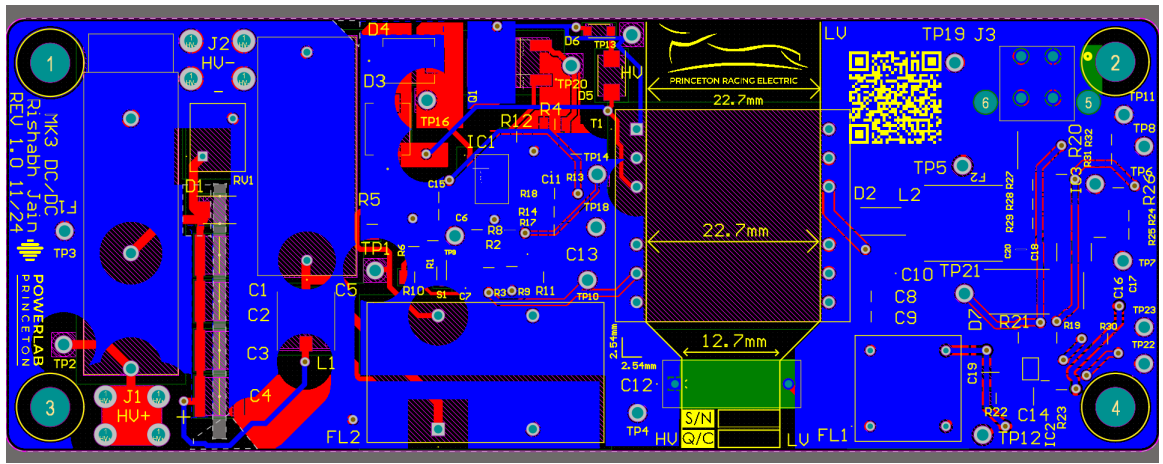


Figure D.3: The bottom copper layer of the PCB.

Appendix E

Bill of Materials

The BOM for this specific project can be accessed on the GitHub as well as here:

[Google Sheet BOM](#)

Bibliography

- [1] *Executive summary – Global EV Outlook 2024 – Analysis*, en-GB. [Online]. Available: <https://www.iea.org/reports/global-ev-outlook-2024/executive-summary> (visited on 12/12/2024).
- [2] L. Fuller-Wright, O. o. C. o. Nov. 2, 2023, and 9. A.m, *The University's electric bus fleet is now rolling*, en. [Online]. Available: <https://www.princeton.edu/news/2023/11/02/princetons-electric-bus-fleet-now-rolling> (visited on 12/12/2024).
- [3] Anjali, *SiC MOSFET in the Automotive Industry — Millennium*, en-US, Jan. 2024. [Online]. Available: <https://www.millenniumsemi.com/blog/how-sic-mosfets-are-transforming-the-automotive-industry/> (visited on 12/12/2024).
- [4] *E-Powertrain Market Report 2024, by Integration Type, Component (Motor, Battery, BMS, Controller, PDM, Inverter/Converter, on-Board Charger), Propulsion (BEV, PHEV), Vehicle Type and Region - ResearchAndMarkets.com*, en, Nov. 2024. [Online]. Available: <https://www.businesswire.com/news/home/20241121859878/en/E-Powertrain-Market-Report-2024-by-Integration-Type-Component-Motor-Battery-BMS-Controller-PDM-InverterConverter-on-Board-Charger-Propulsion-BEV-PHEV-Vehicle-Type-and-Region---ResearchAndMarkets.com> (visited on 12/12/2024).

- [5] *Why More Voltage Makes for Better EVs*, en-US, Section: Car Culture, Aug. 2023. [Online]. Available: <https://www.roadandtrack.com/car-culture/a44794463/why-more-voltage-makes-for-better-evs/> (visited on 12/12/2024).
- [6] *Future Ford EVs Could Utilize 800V Architecture*, en-US, Feb. 2024. [Online]. Available: <https://fordauthority.com/2024/02/future-ford-evs-could-utilize-800v-architecture/> (visited on 12/12/2024).
- [7] *Owner's Manual*, en-US, Tesla Owners Manual. [Online]. Available: <https://www.tesla.com/ownersmanual/> (visited on 12/12/2024).
- [8] *Tesla Batteries: What Kind of Battery Does My Tesla Have?* en-US, Jul. 2023. [Online]. Available: <https://www.findmyelectric.com/blog/what-kind-of-battery-does-my-tesla-have/> (visited on 12/12/2024).
- [9] *Ford LFP Batteries Expected to be Standard Range...* en-US, Feb. 2023. [Online]. Available: <https://www.lightningowners.com/threads/ford-lfp-batteries-expected-to-be-standard-range-replacements.3420/> (visited on 12/12/2024).
- [10] *2025 Hyundai IONIQ 6 Features & Specs — Hyundai USA*, en. [Online]. Available: <https://www.hyundaiusa.com/us/en/vehicles/ioniq-6/compare-specs> (visited on 12/12/2024).
- [11] A. Dhage, *Rivian R1T Battery Pack Benchmarking*, en-US, Jan. 2023. [Online]. Available: <https://www.batterydesign.net/rivian-r1t/> (visited on 12/12/2024).
- [12] *[Battery 101] NMC vs LFP (chemistry, differences, charging habits, reality etc.)* en-US, Jun. 2024. [Online]. Available: <https://www.rivianforums.com/forum/threads/%F0%9F%94%8B-battery-101-nmc-vs-lfp-chemistry-differences-charging-habits-reality-etc-%F0%9F%94%8B.29408/> (visited on 12/12/2024).

- [13] *Taycan Forum - Battery Question*, en-US, May 2024. [Online]. Available: <https://www.taycanforum.com/forum/threads/dumb-battery-question.19882/> (visited on 12/12/2024).
- [14] *Taycan, Taycan 4S, Turbo and Turbo S – The battery - Porsche Taycan*. [Online]. Available: <https://media.porsche.com/mediakit/taycan/en/porsche-taycan/die-batterie> (visited on 12/12/2024).
- [15] *Princeton Racing Electric*, en-US. [Online]. Available: <https://princetonracingelectric.com/awards> (visited on 12/12/2024).
- [16] *Challenges — Formula Hybrid*. [Online]. Available: <https://www.formula-hybrid.org/challenges> (visited on 12/12/2024).
- [17] *EV Handbook - Skid Pad - FSAE*. [Online]. Available: <https://www.fsaeonline.com/Page.aspx?pageid=f7482a82-8d4c-4b30-b151-0ca578e9449a> (visited on 12/12/2024).
- [18] D. Yang, *High Performance Lithium-Ion Battery Design for a Formula Electric Vehicle*, Apr. 2023.
- [19] *Rules and Deadlines*, en. [Online]. Available: <https://drive.google.com/drive/folders/1wQt10w1vQZ09Khxq5INKgEApLvVv1tpw> (visited on 12/12/2024).
- [20] *2025 Formula SAE Rules V.1 are now available*. [Online]. Available: <https://www.fsaeonline.com/cdsweb/app/NewsItem.aspx?NewsItemID=379e4a8a-80a2-4a74-87c2-6f2de4212270> (visited on 12/12/2024).
- [21] *IRH-12/21-W80NB-C—Isolated DC-DC converter—Power Products—Murata Manufacturing Co., Ltd.* [Online]. Available: <https://www.murata.com/en-us/products/productdetail?partno=IRH-12%2F21-W80NB-C> (visited on 12/13/2024).
- [22] D. Simone, *Design of a Universal Compact Low Voltage Vehicle Control Unit for Formula Electric Vehicles*, Apr. 2024.

- [23] C. Lam, *Subject: Re: Questions about your car*, Email sent to Rishabh Jain, Dec. 2024.
- [24] C. Schuster and E. Bender, *Documents – Wisconsin Racing - WR-223E Documentation*, en-US. [Online]. Available: <https://www.wisconsinracing.org/e-documents/> (visited on 12/12/2024).
- [25] *HVI/doc/HVI Schematic.pdf at main · Rootthecause/HVI*, en. [Online]. Available: <https://github.com/Rootthecause/HVI/blob/main/doc/HVI%20Schematic.pdf> (visited on 12/13/2024).
- [26] *FSAE Michigan 2024 Results*, en. [Online]. Available: <https://www.sae.org/site/attend/student-events/formula-sae-michigan/awards-results> (visited on 12/12/2024).
- [27] *2024 – Formula Hybrid Competition Results*. [Online]. Available: <https://www.formula-hybrid.org/history/2024> (visited on 12/12/2024).
- [28] R. Curtin, *Subject: Re: Questions about your car*, Email sent to Rishabh Jain, Dec. 2024.
- [29] B. Glen, *Subject: Re: Quick questions about zips racing's car/tsal*, Email sent to Rishabh Jain, Dec. 2024.
- [30] E. Wu, *Subject: Re: Quick questions about cmu racing's car/tsal*, Email sent to Rishabh Jain, Dec. 2024.
- [31] J. Ares, “Building a smarter ultra-wide DC-DC converter solution with multiple parts,” en,
- [32] A. Kamath, “Push-pull converter simplifies isolated power supply design in HEV/EV systems,” en, 2020.

- [33] T. Hudson, *Understanding LLC Operation (Part I): Power Switches and Resonant Tank — Article — MPS*. [Online]. Available: <https://www.monolithicpower.com/learning/resources/understanding-llc-operation-part-i-power-switches-and-resonant-tank> (visited on 12/13/2024).
- [34] *Integrated Circuits (ICs) — Power Management (PMIC) — Power Supply Controllers, Monitors*, en-us. [Online]. Available: <https://www.digikey.com/en/products/filter/pmic/power-supply-controllers-monitors/760?s=N4IgjCBcpTA7FUBjKAZAhgGwM4FMAaEAeygGORYBWANjbqpCNjrgGYQBdIgBwBcoIAMp8ATgEsAd> (visited on 12/13/2024).
- [35] *Power Designer*. [Online]. Available: <https://webench.ti.com/power-designer/switching-regulator?powerSupply=0> (visited on 12/13/2024).
- [36] *5050 SMD LED - 625nm Red Surface Mount LED with 120 Degree Viewing Angle - Red 5050 SMD LED*, en, Jan. 2020. [Online]. Available: <https://www.superbrightleds.com/5050-smd-led-625nm-red-surface-mount-led-with-120-degree-viewing-angle-red-5050-smd-led> (visited on 12/13/2024).
- [37] B. A. Gilbert Brian, *EMC Filters Comparison Part II: and T Filters*, en-US, Jan. 2020. [Online]. Available: <https://incompliancemag.com/emc-filters-comparison-part-ii-%CF%80-and-t-filters/> (visited on 12/13/2024).
- [38] *LT8316 Datasheet and Product Info — Analog Devices*. [Online]. Available: <https://www.analog.com/en/products/lt8316.html> (visited on 12/13/2024).
- [39] Y. Yang and W. Xiong, *Extending the Supply Voltage of a 600 V Input, No-Optocoupler Isolated Flyback Controller to 800 V or Higher — Analog Devices*. [Online]. Available: <https://www.analog.com/en/resources/design-notes/extending-the-supply-voltage-of-a-600-v-input-no-optocoupler-isolated-flyback-controller.html> (visited on 12/13/2024).

- [40] O. N. Dahl, *MOSFET Gate Resistor*, en-US, Aug. 2021. [Online]. Available: <https://www.build-electronic-circuits.com/mosfet-gate-resistor/> (visited on 12/13/2024).
- [41] H. Anguheven, *Wurth Elektronik Web Chat, 750317464 Interwinding capacitance / 003014470 External*, Nov. 2024.
- [42] *BD9555FVM-C - Data Sheet, Product Detail — ROHM.com*. [Online]. Available: <https://www.rohm.com/products/clocks-and-timers/cr-control-timer-ics/bd9555fvm-c-product> (visited on 12/13/2024).
- [43] *MPQ24833-B*, en. [Online]. Available: <https://www.monolithicpower.com/en/mpq24833-b.html> (visited on 12/13/2024).
- [44] *Conversion Calculator PCB Trace Width*, en-us. [Online]. Available: <https://www.digikey.com/en/resources/conversion-calculators/conversion-calculator-pcb-trace-width> (visited on 12/14/2024).
- [45] *PCB Trace Spacing Calculation for Voltage Levels*. [Online]. Available: <https://www.smps.us/pcbtracespacing.html> (visited on 12/14/2024).